Research Square

Preprints are preliminary reports that have not undergone peer review.
They should not be considered conclusive, used to inform clinical practice,
or referenced by the media as validated information.

Root Water Relations Drive Polystyrene Microplastic-Induced Phytotoxicity in Cucurbita moschata

Somrhita Pal
Brainware University
Sanjukta Dasgupta
Brainware University
Mamon Bala
Brainware University
Sneha Ghosh
Brainware University
Priyanka Sen Guha
Brainware University
Nirlipta Saha
nirlipta.edu@gmail.com

Brainware University https://orcid.org/0000-0001-9649-3863

Research Article

Keywords: Polystyrene microplastics (PSMP), oxidative stress, phytotoxicity, relative water content, soil contamination, food safety

Posted Date: October 30th, 2026

DOI: https://doi.org/10.21203/rs.3.rs-11348188/v1

License: This work is licensed under a Creative Commons Attribution 4.0 International License.
Read Full License

Root Water Relations Drive Polystyrene Microplastic-Induced Phytotoxicity in *Cucurbita moschata*

ABSTRACT

Microplastics (MPs) are emerging contaminants of agricultural soils but their phytotoxic mechanisms under realistic terrestrial conditions remain poorly understood because most studies have been conducted in hydroponic systems. In this study, *Cucurbita moschata* was grown in a soil-like substrate and exposed to 100 nm Polystyrene microplastics (PSMPs), with different doses (0, 0.1, 0.3, and 0.5 mg mL^{-1}) to investigate their effects on plant growth, water relations, stomatal characteristics, photosynthetic pigments, oxidative stress, antioxidant responses, secondary metabolism, and root ultrastructure. PSMP exposure caused a concentration-dependent decline in relative water content (RWC), stomatal pore width, chlorophyll content, and plant growth. Scanning electron microscopy revealed progressive particle accumulation on the root surface at lower concentrations, with vascular localization only at the highest concentration, indicating increasing impairment of root water uptake. Oxidative stress increased with PSMP exposure, as reflected by elevated H_2O_2 and lipid peroxidation, while antioxidant enzymes and phenylpropanoid metabolites were progressively induced but became insufficient to prevent oxidative damage under severe stress. Multivariate data analysis model, Partial Least Squares–Discriminant Analysis (PLS-DA) further supported these responses. It identified water status, antioxidant defense, and growth as the principal processes differentiating PSMP-treated plants from controls. Taken together, the findings identified disruption of root water relations as the primary physiological driver of PSMP phytotoxicity which initiated a cascade of stomatal regulation, photosynthetic dysfunction, oxidative imbalance, and growth inhibition. This study provides a mechanistic framework for predicting the impacts of microplastic contamination on crop productivity under realistic agricultural conditions.

Keywords: Polystyrene microplastics (PSMP), oxidative stress, phytotoxicity, relative water content, soil contamination, food safety.

1. INTRODUCTION

Plastics are synthetic polymers whose production has risen from roughly 2 million metric tonnes in 1950 to more than 390 million tonnes annually, with production expected to exceed 1.1 billion tonnes per year by 2050 (Kochanek et al. 2025). Plastics do not readily biodegrade, they fragment under weathering, UV exposure, and physical wear into microplastics (<5 mm) and, at the smallest end of that range convert into nanoplastics (<1 μm) (Cunningham et al. 2023; Iqbal et al. 2022). An estimated 91% of plastic waste is never recycled and ultimately enters rivers, oceans, and soils (Islam 2025), and micro/nanoplastics have now been detected in most environment, including agricultural soils (Kochanek et al. 2025; Jadhav & Medyńska-Juraszek 2024). A meta-analysis across 89 studies and 553 sites have reported a global mean soil concentration of 2,900 ± 7,600 microplastic items kg^{-1} (Wrigley et al. 2024). The terrestrial plastic contamination that has been estimated at roughly 23 times that of ocean environments (Kochanek et al. 2025) is driven by mulch films, biosolids, contaminated irrigation water, and atmospheric deposition.

Several reports have shown that plants can take up micro/nanoplastics through root hair pores, endocytosis at the root tip, and crack-entry at lateral root junctions, with subsequent movement into stems, leaves, and in some cases fruit (Conti et al. 2020, Bai et al. 2024). Because agricultural soils support most of the global food production, soil associated exposure is of particular concern for food-crop physiology and, potentially, for the food chain. Polystyrene (PS) is repeatedly identified as a dominant polymer in agricultural soils by FTIR-based surveys and in some cases accounting for most detected polymers together with polypropylene (Rathikannu et al. 2025). PS degradation products include styrene which is an IARC Group 2B possible human carcinogen (Zantis et al. 2023).

There were multiple reports that had characterized PS micro/nanoplastic phytotoxicity across several food crops, like growth suppression in lettuce (Hua et al. 2024), wheat (Riaz et al. 2025), rice (Zhang et al. 2021), and other species (Gong et al. 2021; Nei et al. 2024; Zhuang et al. 2023); reductions in chlorophyll and carotenoid content in lettuce, barley, and tomato (Xiao et al. 2024; Liu et al. 2025; Li et al. 2024); and oxidative-stress-linked responses

more broadly (Zantis et al. 2023; Huang et al. 2023; Adhikari et al. 2025; Li et al. 2020). Most of this evidence, however, comes from hydroponic or agar-based exposure systems, which do not reproduce rhizosphere-mediated uptake in a soil-like matrix. Within the Cucurbitaceae these physiological data remain comparatively limited. It is a family that includes Cucurbita spp. (pumpkin/squash), a nutritionally and economically important crop grown on roughly 3 million hectares worldwide (Hosen et al. 2021) and documented as a hyperaccumulator of soil contaminants owing to its high-water demand and extensive root system (Colzi et al. 2022). A pot-grown study of Cucurbita pepo exposed to several conventional microplastic types (polypropylene, polyethylene, PVC, PET) has previously reported effects on growth, photosynthetic performance, and elemental composition (Colzi et al. 2022), however, to our knowledge, no published study has combined water-relations, stomatal-morphometric, photosynthetic-pigment, phenylpropanoid, antioxidant, biochemical, and SEM-based ultrastructural evidence within a single soil-like exposure system specifically for polystyrene nanoplastics in *Cucurbita moschata.*

In comparison to hydroponic/agar systems, soil-like (substrate-based) Polystyrene microplastics (PSMP) exposure systems for Cucurbita are still uncommon. Additionally, despite Cucurbita's recognition as a soil-contaminant hyperaccumulator (Mierzejewska-Sinner et al. 2024), its water-relations, stomatal, and antioxidant responses specifically to PSMP have not been characterized in an integrated design. Besides that, existing single-endpoint or narrow-endpoint studies in other species make it difficult to judge how water status, stomatal behavior, pigment composition, and oxidative/antioxidant biochemistry change together, within one plant, across a concentration series This information is useful for identifying the concentration range over which physiological adjustment gives way to biochemical damage.

Machine learning has emerged as an efficient computational approach for analyzing complex datasets and identifying patterns in environmental research (Liu et al., 2022). Several studies have applied machine learning to microplastic (MP) research, including MP identification, prediction of MP abundance, and forecasting of MP behavior (Chakraborty et al., 2024; Hu et al., 2024; Zhen et al., 2023). However, the application of machine learning to investigate MP-induced responses in plant systems remains limited. Integrating multivariate approaches with physiological and biochemical measurements may therefore provide a useful framework for identifying the key parameters associated with MP-induced phytotoxicity and for improving the prediction of plant responses to MP exposure.

The present study aimed at measuring vegetative growth, relative water content, stomatal morphology, photosynthetic pigments, phenylpropanoid metabolites, oxidative-stress markers, and antioxidant enzyme activities in *Cucurbita moschata* (Indian Pumpkin, Kaddu) exposed to three concentrations of 100 nm PSMP (0.1, 0.3, and 0.5 mg mL^{-1}) in a soil like substrate under polyhouse conditions. Root and stem cross-sections were also examined by SEM to look for particulate structures consistent with PSMP accumulation. Machine learning analyses were performed to integrate and characterize the overall physiological and biochemical responses of Indian pumpkin to PSMP exposure. The aim was to characterize how these physiological and biochemical parameters change together across the concentration series and to find the approximate range over which compensatory antioxidant responses give way to disruption of root water relations leading to downstream photosynthetic impairment, oxidative stress, antioxidant responses, and growth inhibition, in a realistic scenario with soil-like substrate.

2. MATERIALS AND METHODS

2.1. Plant material

Cucurbita moschata (Indian Pumpkin, Kaddu) was used for its rapid growth, widespread agricultural use, and reported sensitivity to environmental stressors. Seeds were sourced from Debgiri Agro Product Private Limited (Barasat, Kolkata) and selected for uniform size and health status prior to sowing. Before sowing, seeds were carefully selected to maintain uniform size and health status, so as to minimize variability and ensure consistency in the experimental results.

2.2 Experimental set up and treatment

The 100 nm PSMPs were obtained from Sigma-Aldrich. A dose-dependent experiment was designed using four PSMP concentrations, 0 (control), 0.1, 0.3, and 0.5 mg mL^{-1} (Maity et al. 2020). The cultivation process began with an overnight soak of the seeds in double-distilled water (ddH_2O), followed by a four-day dark incubation at room temperature to ensure uniform germination. Once germinated, healthy seedlings were moved into rectangular trays

(144 inch^3 volume) filled with a soil-like substrate made of peat and vermiculite (Brooking et al. 1976), with 9 plants each, i.e. 18 plants per treatment (Fig.1). The treatment was performed on 15-day-old seedlings, 2mL of the respective PSMP solution was administered directly to the base of each plant via a precision spray to ensure localized exposure; this process was repeated after every 17 days for a total of three treatments. All plants were grown under polyhouse conditions (35 ± 2°C Day / 26 ± 2°C night) and irrigated with distilled water according to soil field capacity (Pignattelli et al. 2020).



Fig 1: *Cucurbita moschata* grown in trays with soil mixture under polyhouse conditions with four different concentrations of microplastic exposure

2.3. Evaluation of seedling growth, relative water content and stomatal observation

Five plants were randomly selected from each treatment and control group. The specimens were carefully uprooted and thoroughly washed to remove all soil particles. Shoot length was measured from the base to the highest leaf node, while root length was recorded from the base to the tip of the primary taproot, to assess plant responses to environmental stressors. Additionally, broadest leaf diameter was also documented to provide a comprehensive growth assessment. Four fully expanded leaves were sampled from 5 separate individuals per treatment. The fresh weight (FW) was recorded immediately upon collection. To reach full cellular hydration for turgid weight (TW) determination, the leaves were soaked in deionized water for approximately 24 hours. Following this, the samples were oven-dried at 60°C for 48 hours to obtain a constant dry weight (DW). These measurements allowed for the calculation of leaf RWC using the formula described by González and González-Vilar (2001):

$$RWC(\%) = \frac{(FW - DW)}{(TW - DW)} \times 100$$

Stomatal morphology was studied using epidermal peel preparations from the abaxial surface of fully expanded leaves, from all treatments (0, 0.1, 0.3 and 0.5mg/ml). Using fine forceps, thin epidermal peels were carefully stripped, mounted on glass slides in distilled water, and observed under 40X magnification of light microscope. An ocular micrometre (ERMA, Japan) was used as a scale. Stomatal aperture was assessed qualitatively; stomatal distribution and guard cell morphology were compared across treatments. The stomatal index (SI) was calculated as-

$$SI = \frac{Stomata}{Stomata + Epidermal\ cells} \times 100$$

2.4. Determination of chlorophyll and carotenoid contents

Chlorophyll a, chlorophyll b, total chlorophyll and carotenoids contents were determined spectrophotometrically following the method of Lichtenthaler (1987) with modifications. Leaf samples weighing 100 mg were ground in 10 ml of chilled 80% acetone with a pre-cooled mortar and pestle to create a fine pulp. The resulting pulp was centrifuged using a CM-12 PLUS Cooling Microfuge (REMI Instruments, India) at a speed of 8000g, at 4 °C for 10 min. The absorbance of the supernatant was recorded against 80% acetone as a blank at wavelengths of 470, 646.8, and 663.2 nm, utilizing LMPS-UV1900 UV-Vis Scanning Spectrophotometer (Labman Scientific) to calculate the levels of chlorophyll and carotenoid.

.

2.5. Estimation of phenolic, flavonoid and flavonol contents

The methanolic extracts of leaf samples were used to determine the phenolic, flavonoid, and flavonol contents. 500mg leaves were homogenized in 5ml chilled 80% methanol, followed by centrifugation at 8000g, at 4°C for 10 min. The Folin-Ciocalteau method (Lin et al. 2007) was used to determine total phenolic content. 0.1ml of leaf extract was mixed with 2.8ml distilled water, 2% sodium carbonate (2 ml), and 50% Folin-Ciocalteau reagent (0.1 ml). After 30 min of incubation at room temperature, the absorbance of the mixture was measured at 750 nm, keeping distilled water as a blank. Gallic acid equivalents (GAE)/gm in mg of leaf fresh weight were used to express the overall phenolic content.

The total flavonoid content was measured using the method given by Zhishen et al. (1999) with slight modification (Biswas et al. 2025). The leaf extract (0.5 ml) was diluted with 2ml of distilled water and combined with 0.15 ml of 5% $NaNO_2$ (Sodium nitrite). After 5 min, 1.5 ml of 10% $AlCl_3$ (Aluminium chloride) was added. After 6 more min, 1ml 1M NaOH (Sodium hydroxide) was added, and the mixture was well combined. Using distilled water as a blank, the mixture's absorbance was measured at 510 nm. The expression for total flavonoid content was mg of rutin equivalents (RE)/gm of leaf fresh weight.

Total flavonol content was determined using aluminium chloride-sodium acetate colorometric method with slight modification (Kumaran et al. 2007, and Biswas et al. 2025). 2% $AlCl_3$ (0.5 ml) and 1.5 ml of 5% Na_2CO_3 (Sodium carbonate) were combined with the leaf extract (0.5ml). For 2.5hrs the mixture was incubated at room temperature. The solution's absorbance was measured at 440nm with distilled water as a blank. The calibration curve was prepared using an ethanol solution of rutin (rutin (0-100 mg mL^{-1}), which was represented as mg of rutin equivalents (RE)/gm of leaf fresh weight.

2.6. Lipid peroxidation assay

To assess the membrane damage, lipid peroxidation in terms of TBARS (Thiobarbituric acid reactive substances) content was measured as mentioned by Du and Bramlage (1992) and Gupta (2018), with a few modifications. 200 mg leaves were crushed in 5 ml chilled 80% ethanol to create the leaf extract, which was then centrifuged at 8000 g rpm, at 4 °C for 10 min. The extract (1 ml) was combined with 20% TCA (trichloroacetic acid) aqueous solution (4 ml) and 0.67% TBA (2-thiobarbituric acid) aqueous solution. After 30 min at 90 °C in a hot water bath, the mixture was cooled on ice. It was centrifuged at 4 °C for 10 min at 8000 g. The absorbance was measured at 600,532 and 440. The concentration of TBARS was given in terms of nmol malondialdehyde (MDA) equivalents/gm of leaf fresh weight.

2.7. Quantification of hydrogen peroxide (H_2O_2)

The H_2O_2 levels were measured spectrophotometrically, following the protocol given by Velikova et al. (2000). Using a chilled mortar and pestle, 500 mg fresh leaves were homogenized in 5 ml ice-cold 0.1% (w/v) TCA. The homogenate was centrifuged at 4 °C for 15 min at 12,000 g. 0.5 ml of supernatant was mixed with 0.5 ml of 10 mM potassium phosphate buffer (pH 7.0) and 1 ml of 1 M KI (potassium iodide). The mixture was incubated in the dark for 1h and the absorbance was measured at 390 nm.

2.8. Estimation of antioxidant enzyme activities

Peroxidase (POD), superoxide dismutase (SOD), and catalase (CAT), activities were measured using the extracts of leaf samples obtained by homogenizing 100 mg leaves in 1 ml of ice cold 100 mM phosphate buffer (pH 7.0) containing 2% PVP (polyvinylpyrrolidone), 1 mM PMSF (phenylmethylsulfonyl fluoride), 0.2% Triton X-100 and 0.1 mM EDTA (ethylenediaminetetraacetic acid). It was followed by centrifugation at 4°C for 20 min at 12,000g. The supernatant was ultimately used as an enzyme extract and the total protein content in the samples was determined using the Bradford assay (Kruger, 2009).

Peroxidase assay (POX) The method adopted by Kar and Mishra (1976) was used to measure POD activity following the conversion of pyrogallol to purpurogallin in the presence of H_2O_2 (hydrogen peroxide) using with slight modifications. 10µl of enzyme extract was added to 5 ml of pyrogallol and phosphate buffer solution, and 50µl of ten-times diluted 30% H2O2. The change in absorbance was recorded at 420 nm for 4 min. Formation of

1µmol purpurogalin per minute was considered as one unit of enzyme activity and was calculated using ε = 2.47 mM−1 cm−1 as the extinction coefficient of purpurogallin at 420 nm.

Super oxide dismutase assay (SOD) SOD activity was assessed according to Beyer and Fridovich (1987) and Gupta (2018) by following the inhibition of formazan formation via NBT reduction. Aliquots of enzyme extract ranging from 50-200µl were added to a 2ml reaction mixture containing 0.1mM Na_2EDTA, 57µM NBT, 9.9mM L-methionine, and 0.9mM L-methionine and 0.9µM riboflavin prepared in 50mM phosphate buffer (pH 7.8). The absorbance was recorded at 560nm. The reaction mixture was exposed to light from a fluorescent light, and the change in absorbance was recorded after 3 minutes. The activity was measured by the amount of enzyme required for inhibition of formazan formation.

Catalase activity (CAT) CAT activity was assessed by the method mentioned by Dutta Gupta and Datta (2003). A reaction mixture containing 1.8 ml 50mM phosphate buffer (pH 7), 100µl of enzyme, and 100µl of 50 times diluted 30% H_2O_2 was prepared. For 3 min, the decrease in absorbance at 240 nm was recorded immediately after preparing the reaction mixture. Decomposition of H2O2 at the rate of 1 µmol/min was considered as one unit of enzyme activity, which was calculated using $\varepsilon = 0.036\ mM^{-1}\ cm^{-1}$ as the extinction coefficient of H_2O_2 at 240 nm.

Ascorbate peroxidase activity (APX) APX activity was determined by the method of Nakano and Asada (1981), monitoring the decrease in absorbance at 290 nm for 3 min. The reaction mixture contained 1 ml of 50 mM phosphate buffer (pH 7.0), 200µl of 1 mM EDTA, 200µl of 5 mM ascorbate, 200µl of enzyme extract and 200µl of 1 mM H2O2, added to initiate the reaction. Decomposition of ascorbate at the rate of 1 µmol/min was considered as one unit of enzyme activity, calculated using $\varepsilon = 2.8\ mM^{-1}\ cm^{-1}$ as the extinction coefficient of ascorbate at 290 nm.

2.9. SEM analysis

To visualize the surface morphology and potential internalization of PS-MPs, root, stem and petiole segments were harvested and fixed in 4% paraformaldehyde (buffered with 0.1 M PBS, pH 7.2) for 24 hours at 4°C. Following fixation, samples underwent systematic dehydration through an ascending acetone gradient (50%, 60%, 70%, 90%, and 100% v/v), with each stage lasting 20 minutes. To preserve structural integrity and osmotic stabilization, the dehydrated samples were air-dried under controlled conditions. The specimens were subsequently mounted onto aluminum stubs using conductive double-sided carbon adhesive tape. A thin, uniform layer of gold was applied via sputter coating (~10 nm) to enhance surface conductivity and minimize charging effects. Observations were conducted using a scanning electron microscope (Zeiss EVO LS10) at an accelerating voltage of 20 kV.

2.10. Statistical analysis

GraphPad Software, San Diego, CA, USA, was used for statistical analysis. All experiments were performed in quadruplets and presented as the mean ± standard error. One-way analysis of variance (ANOVA) and LSD Fisher test at $p < 0.05$, were employed to examine the significant variance between the treated and control groups (Xiao et al. 2024). The Pearson correlation 197 coefficients was used to assess correlation between the observation between %RWC and Stomatal pore (Gholampoor et al.,2025).

2.11. Machine learning based analysis

To evaluate the overall physiological and biochemical responses of Indian pumpkin to PSMP exposure, multivariate statistical analyses were performed. The dataset comprised 12 biological samples, including control plants and PSMP-treated plants, with physiological, biochemical, and antioxidant parameters used as input variables. Prior to analysis, the data were normalized by autoscaling (mean-centering followed by division by the standard deviation) to minimize differences in variable scales.

Hierarchical clustering analysis (HCA) was conducted using Euclidean distance and Ward's linkage method to visualize similarities among samples and identify clustering patterns based on their physiological and biochemical profiles. A heatmap was generated to illustrate the relative abundance of each variable across all samples.

Partial Least Squares–Discriminant Analysis (PLS-DA) was subsequently performed to evaluate class separation between control and PSMP-treated plants. Variable Importance in Projection (VIP) scores were calculated to identify the variables contributing most to group discrimination. Variables with VIP scores greater than 1 were considered important biomarkers associated with PSMP-induced phytotoxicity.

3. RESULTS AND DISCUSSION

3.1. Effects of Microplastics on plant growth

The impact of the different concentrations of PSMP on the morphological parameters of the Cucurbita plant was analysed. Root length and shoot length both declined with increasing PSMP concentration, but the reduction reached statistical significance only at 0.5 mg mL^{-1} (~25–26% below control; $P < 0.05$), with 0.1 and 0.3 mg mL^{-1} statistically indistinguishable from control. However, leaf area followed a modest, non-significant decline at 0.1 mg mL^{-1} (~8%), an intermediate response at 0.3 mg mL^{-1} overlapping statistically with both neighbouring groups, and a significant reduction (~20%) only at 0.5 mg mL^{-1} (Figure 2). RWC, by contrast, declined significantly and monotonically across the entire concentration series, with every treatment significantly different from every other (control > 0.1 > 0.3 > 0.5 mg mL^{-1}; $P < 0.05$) with a 34% reduction at 0.1 mg mL^{-1}, 44% at 0.3 mg mL^{-1}, and 68% at 0.5 mg mL^{-1} relative to control (Fig. 3).

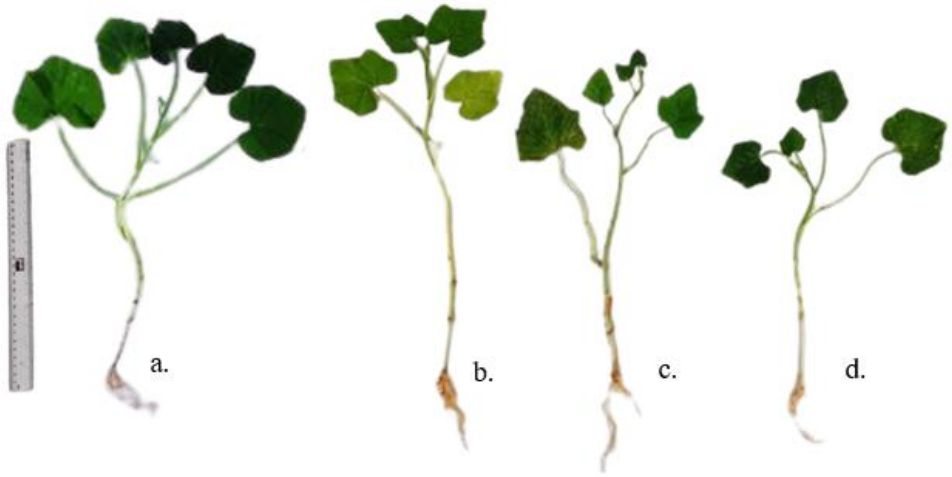


Fig 2: After 51days of growth, the morphological features of plants treated with different concentrations of PSMP- a. 0 (control) mg mL^{-1}, b. 0.1mg mL^{-1}, c. 0.3 mg mL^{-1}, and d. 0.5 mg mL^{-1}. Scale-15cm

From these observations, it was understood that although RWC declined progressively across all PSMP treatments, growth inhibition became significant only at 0.5 mg mL^{-1} thereby indicating that growth was protected against moderate reductions in water status. This non-linear response is consistent with the turgor-threshold model. Instead of declining proportionally with water loss, the cell expansion is maintained until turgor pressure falls below the minimum threshold required for irreversible cell wall extension (Hsiao et al., 2000; Ortega, 2025). Even though the leaf area showed non-significant reduction at 0.1 mg mL^{-1} at the earlier stage, no change was seen in root or shoot length. This shows that leaf expansion is more sensitive to water deficit and can serve as an early indicator of impaired growth before noticeable reductions in photosynthesis occur (Tardieu, 2024). The early decline in RWC, even at the lowest PSMP concentration, is likely related to impaired water uptake caused by particle accumulation around the root surface. These observations were later supported by SEM analysis. This transition from surface association to vascular internalization agrees with the threshold-like growth inhibition observed at the highest concentration. Similar dose-dependent shifts from external adsorption to internal penetration have been reported for polystyrene nanoplastics in *Allium cepa* (Giorgetti et al., 2020) and are consistent with evidence that root cell walls and apoplastic barriers initially restrict nanoplastic entry, with vascular penetration occurring only after these exclusion mechanisms are overwhelmed (Bosker et al., 2019; Zhu et al., 2022; Maity et al., 2024; Xu et al., 2025; Ramachandran et al., 2025).

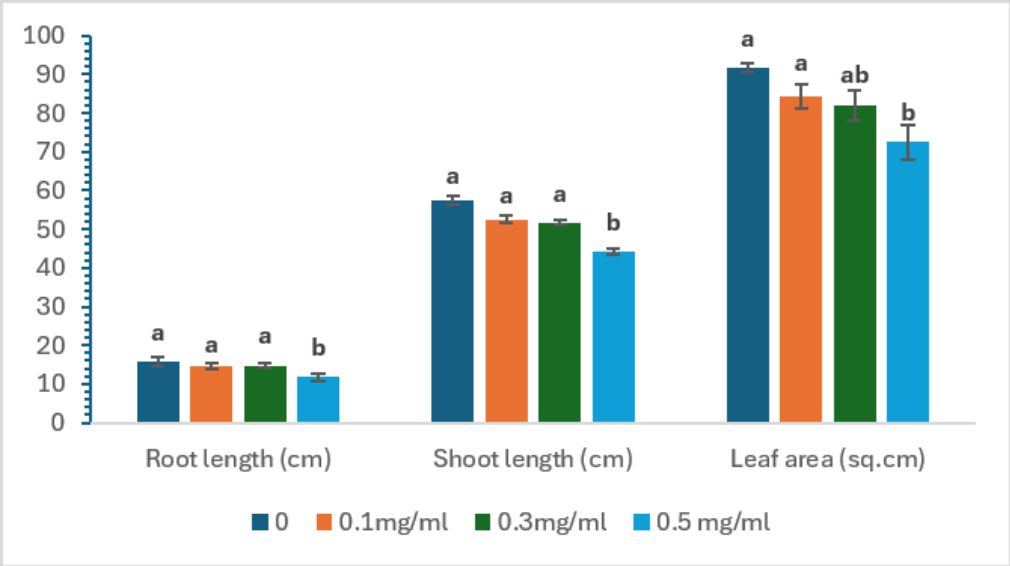


Fig 3: Effect of PSMP on root length (cm), shoot length (cm), and leaf area (cm²) in pumpkin. Different lowercase letters indicate significant differences according to the LSD Fisher test ($p < 0.05$).

These findings are consistent with recent reviews identifying root-surface pore blockage as a primary mechanism by which microplastics impair plant water status before internalization occurs (Jia et al., 2023; Wang F. et al., 2022; Kumar et al., 2024). This interpretation is further supported by the exploratory PLS-DA, which identified RWC as one of the most influential variables distinguishing PSMP-treated plants from controls. The distinction of RWC as the highest-ranking variable marks its importance as the first physiological indicator of PSMP stress, and leaf area reflects the downstream consequences of sustained water limitation. These multivariate findings are fully consistent with the univariate responses observed in the present study, suggesting that impaired water status precedes significant growth inhibition (Fig.4).

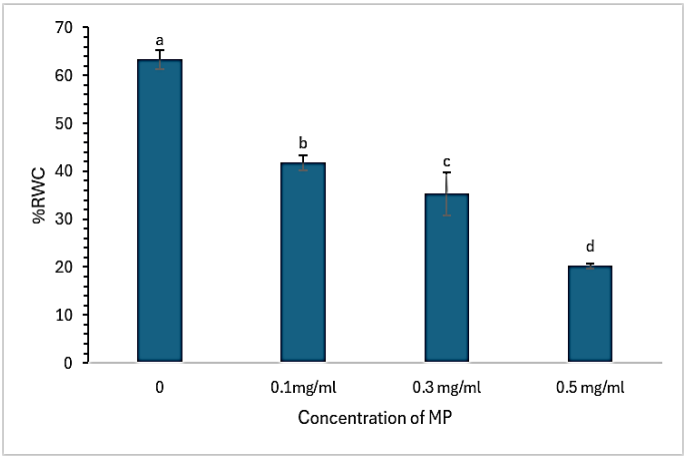


Fig 4: Relative water content (% RWC) in pumpkin leaves under PSMP stress. Different lowercase letters indicate significant differences according to the LSD Fisher test ($p < 0.05$).

3.2. Effects of microplastics on stomatal morphology and characteristics

Abaxial epidermal peels showed clear, concentration-dependent changes in stomatal morphology across all PSMP treatments. The morphological change in the treated stomatal cells is shown in Fig. 5. Control plants involved the widest stomatal pore followed by longest guard cells and highest stomatal index. Pore width and guard-cell length declined significantly with dose, falling to a reduction of 61.85% and 26.25% at 0.5 mg mL^{-1}, respectively. Stomatal

index (SI) declined from 19.15% to 4.35% over the same range (77.3% reduction). Pore width correlated strongly with %RWC across the series (r = 0.981, p = 0.019) (Fig.6).

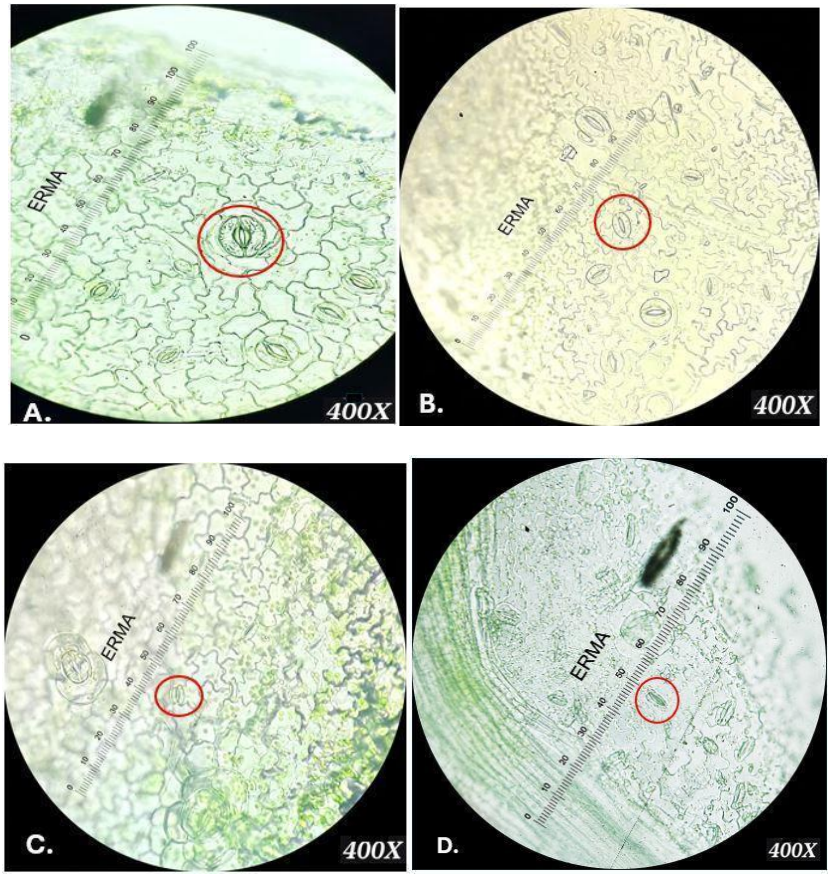
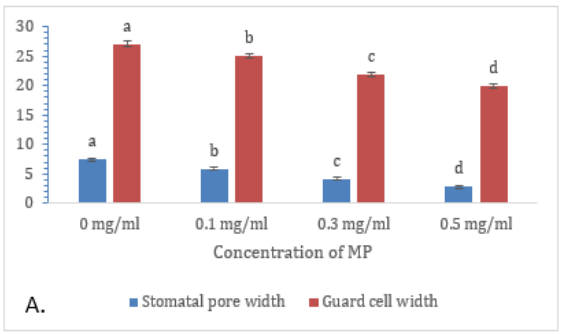


Fig 5: Light micrographs (400X) of abaxial epidermal peels of *Cucurbita moschata* showing stomatal morphology under soil PSMP exposure: A. Stomata with wide aperture in control plants, B. Stomata partially closed 0.1mg/ml MP, C. Stomata with narrow aperture in 0.3mg/ml MP treated plants, and D. Stomata with collapsed guard cells with 0.5mg/ml MP. Scale: 1 ocular division= 3.33µm.



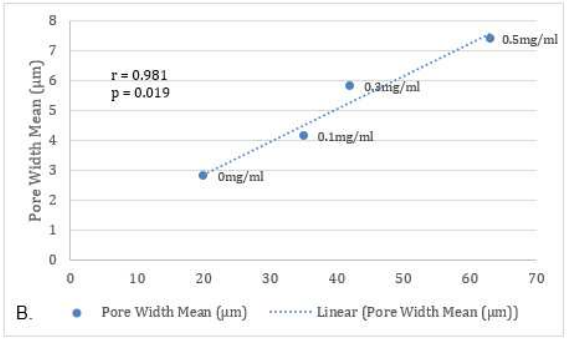


Fig 6: A. Stomatal response in pumpkin leaves under different concentrations of PSMP stress**.** Different lowercase letters indicate significant differences according to the LSD Fisher test ($p < 0.05$). B. Correlation with % RWC and Stomatal pore width

This progressive reduction in stomatal pore width is consistent with an active response to declining plant water status. According to several studies, ABA-mediated stomatal closure under water deficit minimizes transpirational water loss and improves intrinsic water-use efficiency (Liu et al., 2022; Yang et al., 2021; Postiglione & Muday, 2020). This simultaneously restricts CO_2 diffusion thereby limiting carbon assimilation and promoting excess excitation energy that can enhance ROS production (Foyer & Hanke, 2022; Parkash et al., 2024). This provides a plausible explanation for the concurrent decline in chlorophyll content and increase in H_2O_2 observed in the present study, although gas-exchange measurements were not performed. Consistent with these observations, polystyrene microplastics have been shown to suppress stomatal conductance and photosynthetic performance more strongly than several other polymer types (Kralj et al., 2026; Zhu et al., 2025). The associated reduction in guard-cell turgor likely also contributed to the growth inhibition observed under PSMP exposure.

The physiological significance of stomatal narrowing was dose dependent. At 0.1 and 0.3 mg mL^{-1}, reduced stomatal aperture coincided with enhanced antioxidant capacity. This is characterized by increased SOD activity, maximal CAT and POD activities, and unchanged MDA levels, thereby indicating effective physiological acclimation. In contrast, at 0.5 mg mL^{-1}, the lowest stomatal index was accompanied by declining CAT and POD activities and a significant increase in MDA, suggesting that antioxidant defences were no longer sufficient to prevent oxidative membrane damage despite continued stomatal regulation. A similar transition from adaptive stomatal regulation to oxidative dysfunction under higher nanoplastic exposure has been reported in lettuce (Ozfidan-Konakci et al., 2023), thus indicating that the dose depended altered water relations observed in this study are connected to stomatal regulation.

3.3. Effects of microplastics on Photosynthetic Pigments

All the photosynthetic pigments studied were found to decline progressively with increasing PSMP concentration (Fig. 7). Compared to the control, chlorophyll *a* was significantly reduced in all PSMP-treated plants. The greatest reduction was however observed at 0.5 mg mL^{-1}. A similar trend was recorded for chlorophyll b and total chlorophyll as well. In contrast, carotenoid content increased progressively with PSMP concentration and reached its highest value at 0.5 mg mL^{-1}. At 0.5 mg mL^{-1} it was significantly higher than that of the control and the lower PSMP treatments, but the intermediate concentrations showed overlapping statistical groups.

The progressive decline in chlorophyll *a*, chlorophyll *b*, and total chlorophyll shows that PSMP exposure diminished chloroplast function and photosynthetic efficiency. Studies have shown that microplastic-induced oxidative stress can inhibit chlorophyll biosynthesis, accelerate pigment degradation, and disrupt photosystem II, which reduces light harvesting and carbon assimilation (Wang et al., 2023). In relation to the decreased RWC and stomatal narrowing observed in the present study, restricted CO_2 availability likely increased excitation pressure within chloroplasts, promoting ROS accumulation and pigment degradation (Foyer & Hanke, 2022; Parkash et al., 2024).

Carotenoid content by contrast, increased gradually with PSMP concentration which indicates activation of a photoprotective response. Carotenoids dissipate excess excitation energy and quench reactive oxygen species to protect the photosynthetic apparatus under stress (Niaz et al., 2023). However, their accumulation was insufficient to prevent chlorophyll loss at higher PSMP concentrations which suggest that oxidative stress eventually exceeded the photoprotective capacity of the antioxidant system. Collectively, these findings indicate that PSMP-induced disruption of plant water status and redox homeostasis compromises photosynthetic performance and ultimately contributes to the observed reduction in plant growth.

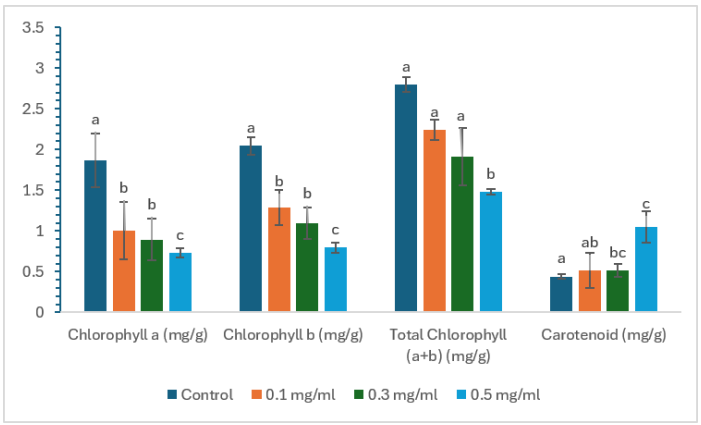


Fig 7: Effect of PS-MPs on chlorophyll a, chlorophyll b, total chlorophyll and carotenoid content (mg g^{-1} FW). Different lowercase letters indicate significant differences according to the LSD Fisher test ($p < 0.05$).

3.4. Effects of microplastics on Total Phenolic (TPC), Flavonoid, and Flavonol

The total phenolics (TPC), flavonoids, and flavonols are all three metabolites of phenylpropanoid pathway and showed significant, dose-dependent changes relative to control (Fig. 8). TPC was significantly reduced at 0.1 mg mL^{-1} and continued decreasing to the highest dose at 0.5 mg mL^{-1}. In contrast, Flavonoid showed a progressive significant increase, from 0.1 mg mL^{-1} to 0.3 and 0.5 mg mL^{-1}. Flavonol also showed the strongest monotonic increase of all three parameters, with significance at 0.1 mg mL^{-1} rising at 0.5 mg mL^{-1}. This indicates that the phenylpropanoid pathway was activated early and sustained across the entire concentration range.
PSMP are known to induce ROS, particularly H_2O_2 which serves as second messengers to trigger this pathway (Ninkuu et al. 2025). These metabolites constitute an important non-enzymatic antioxidant system that complements enzymatic ROS detoxification. They scavenge excess free radicals and contribute to cellular redox homeostasis (Rao et al., 2025; Daryanavard et al., 2023). Similar activation of phenylpropanoid metabolism has been reported in cucumber, *Ginkgo biloba*, and *Tetrastigma hemsleyanum* exposed to polystyrene micro- and nanoplastics, where increased flavonoid accumulation was associated with enhanced stress tolerance (Liu et al., 2024; Cui et al., 2025; Xie et al., 2026). The decline in total phenolic content (TPC) does not necessarily contradict this response. Instead, it may reflect selective metabolic reallocation towards flavonoid and flavonol biosynthesis rather than uniform accumulation of all phenolic compounds. Such a shift has already been previously reported under abiotic stress (Caldo et al., 2025). Such metabolic prioritization would explain the concurrent increase in flavonoids and flavonols despite reduced TPC under PSMP exposure. These stress responses are consistent with reduced photosynthetic performance following impaired stomatal function observed in this study.

3.5. Effects of microplastics on Hydrogen Peroxide (H_2O_2) and Lipid Peroxidation

Both H_2O_2 and Lipid peroxidation are indicators of oxidative stress. In this study, compared to control, H_2O_2 content increased significantly and progressively across all PSMP concentrations (Fig. 8). Significant elevation was observed from 0.1 mg mL^{-1} and reaching up to 0.3 and 0.5 mg mL^{-1}. Lipid peroxidation expressed in terms of MDA content, showed a non-monotonic response (Fig. 8). At 0.1 and 0.3 mg mL^{-1}, MDA was not significantly elevated relative to control. However, at 0.5 mg mL^{-1} MDA increased significantly, demonstrating that membrane lipid oxidation becomes significant only at the highest PSMP dose.
This accumulation of H_2O_2 levels with increasing dosage is the link between the stress imparted by PSMP and all subsequent biological reactions observed. The absence of significant MDA accumulation at 0.1 and 0.3 mg mL^{-1}, despite significant H_2O_2 elevation at these concentrations can be interpreted as evidence that the antioxidant defense system, the enzymatic SOD, CAT, POD pathway and non-enzymatic phenolics, flavonoids, flavonols, carotenoids pathway is sufficiently activated at low-to-moderate doses to prevent H_2O_2 from reaching membrane lipids in damaging quantities. Studies by Zantis et al. (2023), Zhang et al. (2021) confirm such progressive H_2O_2 accumulation in plant cells under PSMP stress, with H_2O_2 serving as a key trigger of the coordinated antioxidant defence response. If not scavenged by antioxidants, ROS can damage cell structures including oxidative deterioration of lipids (lipid

peroxidation) eventually leading to cell death (Zantis et al. 2023). The MDA data thus provides functional evidence that antioxidant protection is effective at 0.1–0.3 mg mL^{-1} but partially fails at 0.5 mg mL^{-1}. Sajjad et al. (2025) studies on wheat (*Triticum aestivum)* and maize (*Zea mays*) showed similar results. Both crops showed reduced growth and chlorophyll, along with increased oxidative damage, raised antioxidant enzymes and proline levels in both plants.

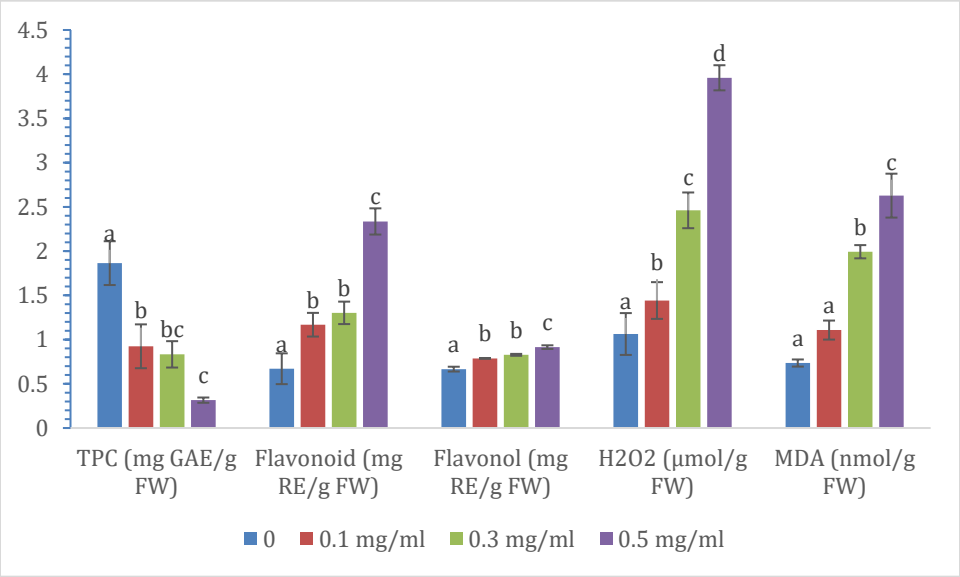


Fig 8: Effect of PSMPs on total phenolics (TPC), flavonoid, flavonol, H_2O_2, and MDA content. Different lowercase letters indicate significant differences according to the LSD Fisher test ($p < 0.05$)

3.6. Effects on Antioxidant Enzymes

Impact on antioxidant enzyme activities in presence of different concentrations of PSMP were studied to understand how the treated plants combat the PSMP induced stress in the Cucurbita cells (Fig. 9). SOD activity increased progressively with PSMP concentration, whereas CAT and POD exhibited a biphasic response, peaking at 0.3 mg mL^{-1} before declining to near-control levels at 0.5 mg mL^{-1}. This coordinated response reflects activation of the antioxidant defence system, with sustained SOD induction indicating continued ROS production under increasing PSMP exposure. Similar trends have been reported in wheat and black mustard exposed to polystyrene micro- and nanoplastics (Riaz et al., 2025; Adhikari et al., 2025).

The transient induction of CAT and POD at 0.3 mg mL^{-1}, together with the absence of significant MDA accumulation, suggests that antioxidant defences were sufficient to maintain redox homeostasis under moderate PSMP stress. However, their decline at 0.5 mg mL^{-1} despite continued increases in SOD and H_2O_2 coincided with significant lipid peroxidation, indicating that ROS production exceeded the detoxification capacity of the antioxidant system. Similar threshold-dependent antioxidant responses have been reported in *Lemna minor*, wheat, and maize under polystyrene microplastic stress (Zhou et al., 2023; Ozfidan-Konakci et al., 2023; Sajjad et al., 2025). APX exhibited a comparatively weaker response, possibly reflecting constraints in the ascorbate–glutathione cycle under prolonged oxidative stress (Adhikari et al., 2025). The prominence of SOD in multivariate analysis further supports its role as a key biochemical marker of PSMP-induced oxidative stress, although the broader implications of the PLS-DA are discussed separately.

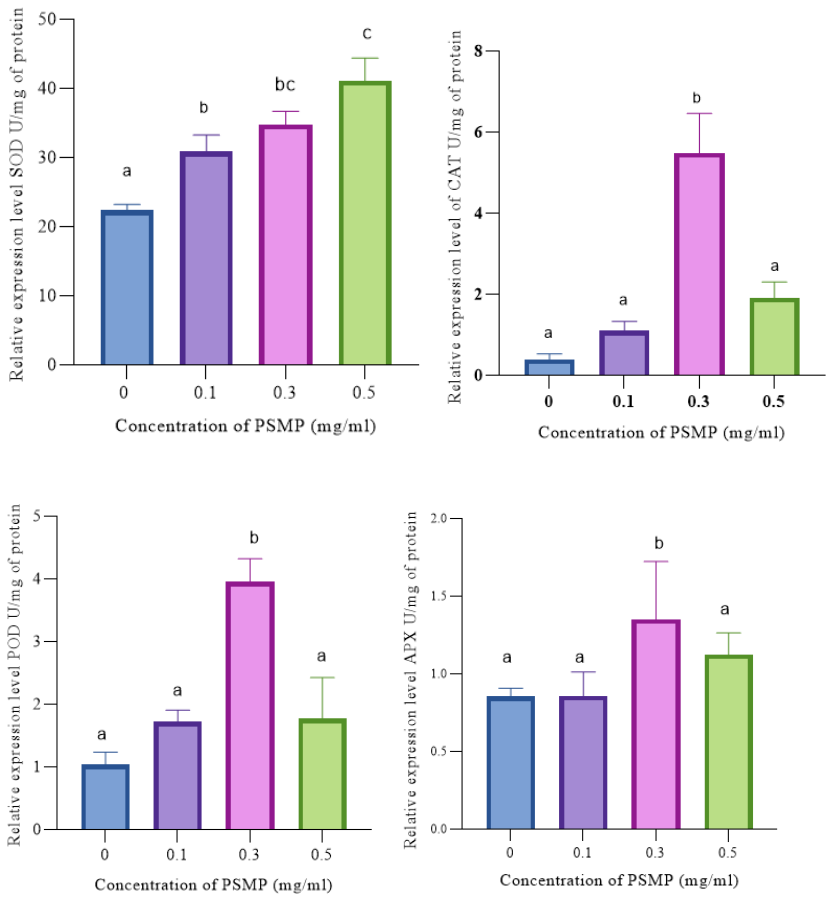
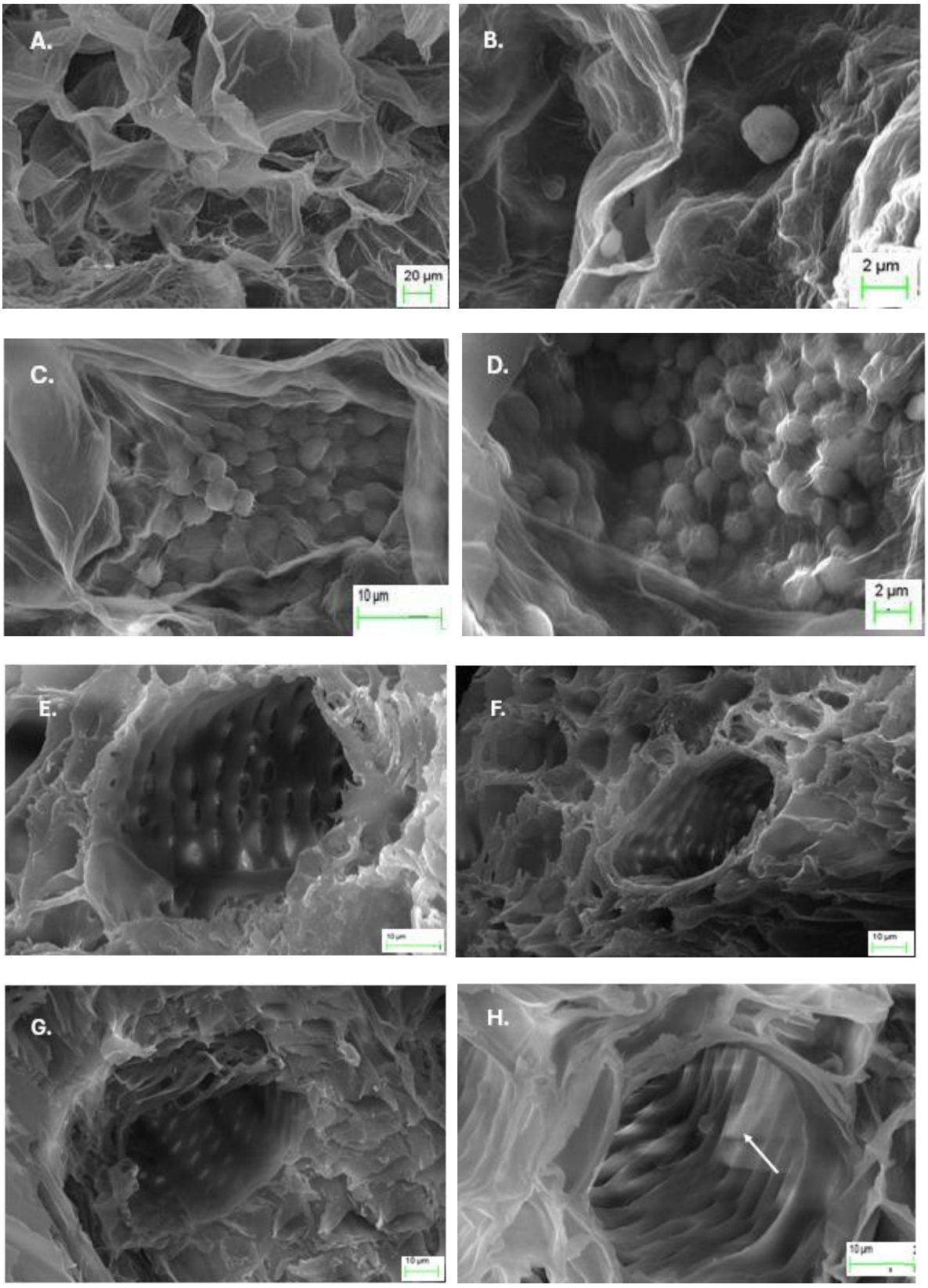


Fig 9: Relative expression level of SOD, CAT, POD and APX under PSMP stress. Different lowercase letters indicate significant differences according to the LSD Fisher test ($p < 0.05$)

3.7. SEM visualization of PSMPs translocation under varying exposure levels

Scanning Electron Microscopy (SEM) provided definitive evidence of the uptake and subsequent internalization of microplastics (MPs) within the plant's vascular system. No PSMP particles were found in the control plants. However, at 0.1 mg mL^{-1} and 0.3 mg mL^{-1}, PSMPs were predominantly confined to the root surface and surrounding substrate (Fig. 10B-D), whereas at 0.5 mg mL^{-1}, particles were also detected within the xylem and adjacent cortical tissues (Fig. 10H). In root cross-sections treated with 0.5 mg mL^{-1}, MPs were clearly sequestered within the xylem vessels and adjacent cortical tissues. This confirms that the root system acts as the primary interface for MP entry, likely through "crack-entry" pathways at lateral root emergence sites or via apoplastic transport through intercellular spaces (Zhou et al. 2023; Li et al. 2023). This study revealed a distinct translocation bottleneck (Fig. 10E-H). While root accumulation was immediate and robust, significant traces were absent in stem tissues at the 51-day mark, suggesting a restricted upward flux governed by vascular transport barriers (Lian et al. 2020). However, by day 70, PSMP accumulation was observed in the stem, indicating that translocation is a time-dependent process (Fig. 10I-L). This delayed migration may be attributed to the gradual bypass of the endodermal barrier or the accumulation of smaller particles that eventually overcome hydraulic resistance within the xylem (Liu et al. 2022). These observations align with documented patterns in lettuce, rice, and *Solanum nigrum*, where particles frequently form "grape-like" aggregates on xylem cell walls (Zhou et al. 2023; Zhang et al. 2021). The internalization of these polymers within the vascular bundles not only facilitated systemic distribution to the leaves but also created the physical basis for the oxidative stress and photosynthesis inhibition observed elsewhere in this study (Li et al. 2023). The internal presence of PSMP in roots treated with 0.5 mg mL^{-1} explained the elevated stress response observed in that plant as compared

to other treatments which showed low to moderate stress responses with PSMP present only at the root surfaces and soil.



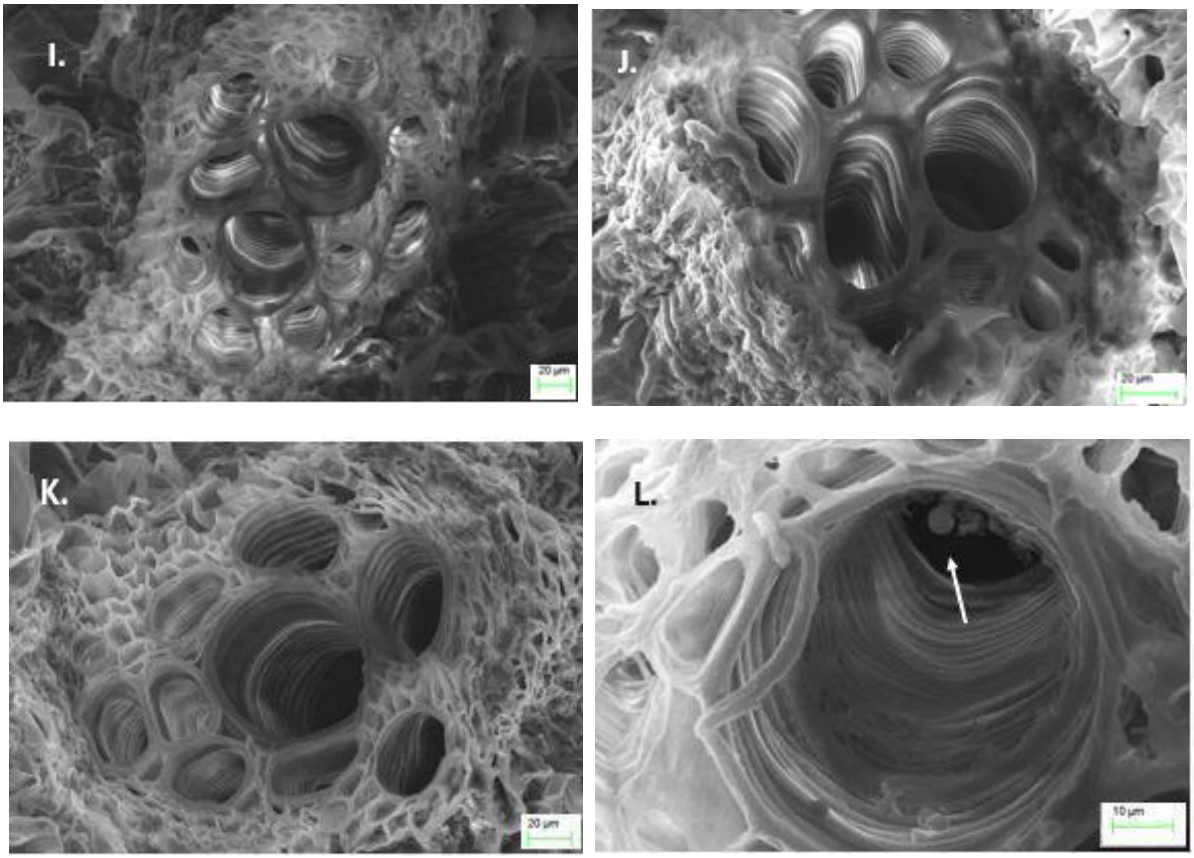


Fig 10: Tissue distribution of 100nm PSMPs in pumpkin roots and stems. SEM images of transverse sections of roots and stems showing the distribution of 100nm PSMPs following exposure to 0,0.1,0.3, and 0.5 mg mL^{-1} PSMPs. (A-D) Root peripheral tissues from control, 0.1,0.3mg mL^{-1} treatments, respectively, showing PSMP accumulation predominantly in the peripheral tissues. (E-H) Root xylem showing no apparent PSMP accumulation in the control, 0.1 and 0.3mg mL^{-1} treatments (E-G), whereas PSMP particles were observed within the xylem at 0.5 mg mL^{-1} (H). (I-L) Stem xylem showing a similar pattern, with no apparent particle accumulation in the control, 0.1 and 0.3mg mL^{-1} treatments (I-K), while particles were observed within the xylem at 0.5 mg mL^{-1}. Scale bars are indicated in each image.

3.8. Machine learning analysis reveals distinct physiological responses to PSMP exposure

Hierarchical clustering analysis revealed clear differences between control and PSMP-treated plants based on their physiological, biochemical, and antioxidant responses (Fig. 11). The heatmap showed that control samples clustered separately from treated samples, indicating distinct response patterns following PSMP exposure (Fig.12). Growth-related parameters, including RWC, chlorophyll pigments, shoot length, root length, and leaf area, were generally higher in control plants, whereas treated plants exhibited relatively higher levels of oxidative stress markers and antioxidant enzymes, including superoxide dismutase (SOD), catalase (CAT), hydrogen peroxide (H_2O_2), lipid peroxidation (MDA), flavonoids, and flavonols. These clustering patterns indicate coordinated physiological and biochemical alterations induced by PSMP stress.

PLS-DA further confirmed the discrimination between control and PSMP-treated samples. The first two latent variables explained 86.9% of the total variance, with Component 1 accounting for 83.1% and Component 2 accounting for 3.8%. A distinct separation of the two groups was observed primarily along Component 1, demonstrating that PSMP exposure produced marked alterations in the physiological and biochemical profiles of Indian pumpkin.

The corresponding Variable Importance in Projection (VIP) analysis identified RWC (VIP = 3.50) as the most influential variable contributing to group discrimination, followed by SOD (VIP = 1.55) and leaf area (VIP = 1.25). All three variables exceeded the commonly used VIP threshold of 1, suggesting that plant water status, antioxidant response, and vegetative growth were the major variables contributing to the observed separation between control and

PSMP-treated plants. In contrast, the remaining variables had VIP scores below 1, indicating comparatively lower contributions to group discrimination within the PLS-DA model.

The multivariate analysis provides an integrated view of the physiological and biochemical responses of Indian pumpkin to PSMP exposure. The prominent contribution of RWC in the PLS-DA model is consistent with its progressive decline across the PSMP concentration gradient, suggesting that water status was particularly sensitive to PSMP exposure (Mousazadehgavan et al. 2026) In contrast, significant reductions in root and shoot growth were observed only at the highest concentration, indicating that alterations in water status occurred before pronounced growth inhibition. The high VIP score of SOD further reflects the importance of antioxidant defence in distinguishing PSMP-exposed plants from controls, consistent with the antioxidant response observed under PSMP stress. Similarly, the contribution of leaf area to group discrimination is consistent with the reduction in leaf area observed at higher PSMP exposure. Collectively, these findings suggest that changes in water status, antioxidant defence, and vegetative growth represent closely associated components of the physiological response to PSMP exposure.

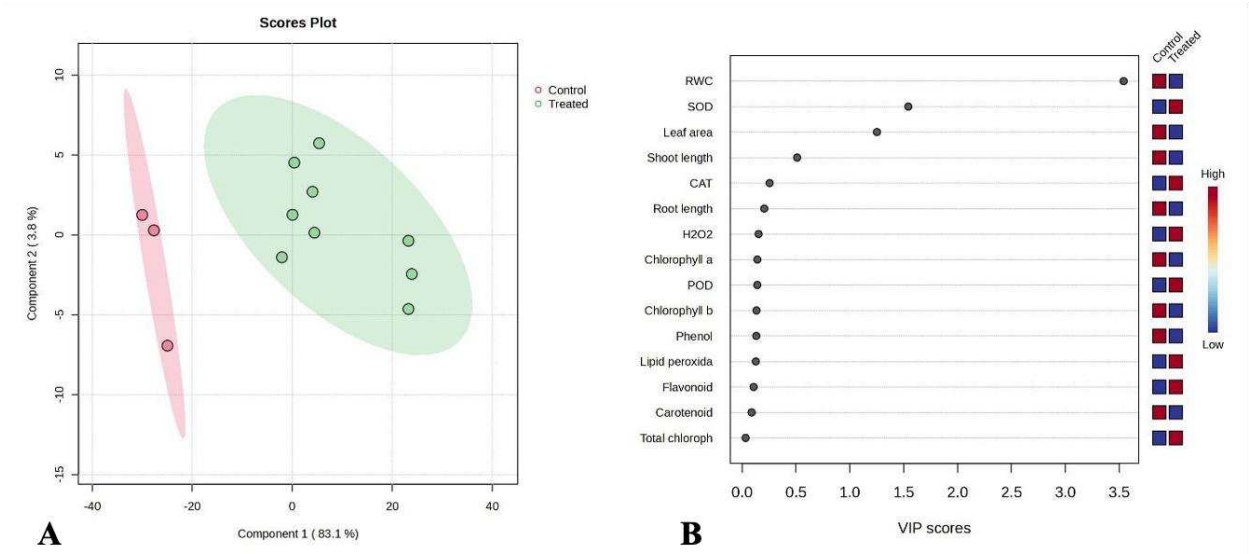


Fig 11: Partial Least Squares–Discriminant Analysis (PLS-DA) of physiological and biochemical responses of Indian pumpkin exposed to PSMPs. (A) PLS-DA score plot showing clear separation between control and PSMP-treated samples. (B) Variable Importance in Projection (VIP) scores identifying the major biomarkers responsible for class discrimination. RWC, superoxide dismutase (SOD), and leaf area exhibited VIP scores greater than 1, indicating their dominant contribution to PSMP-induced phytotoxicity.

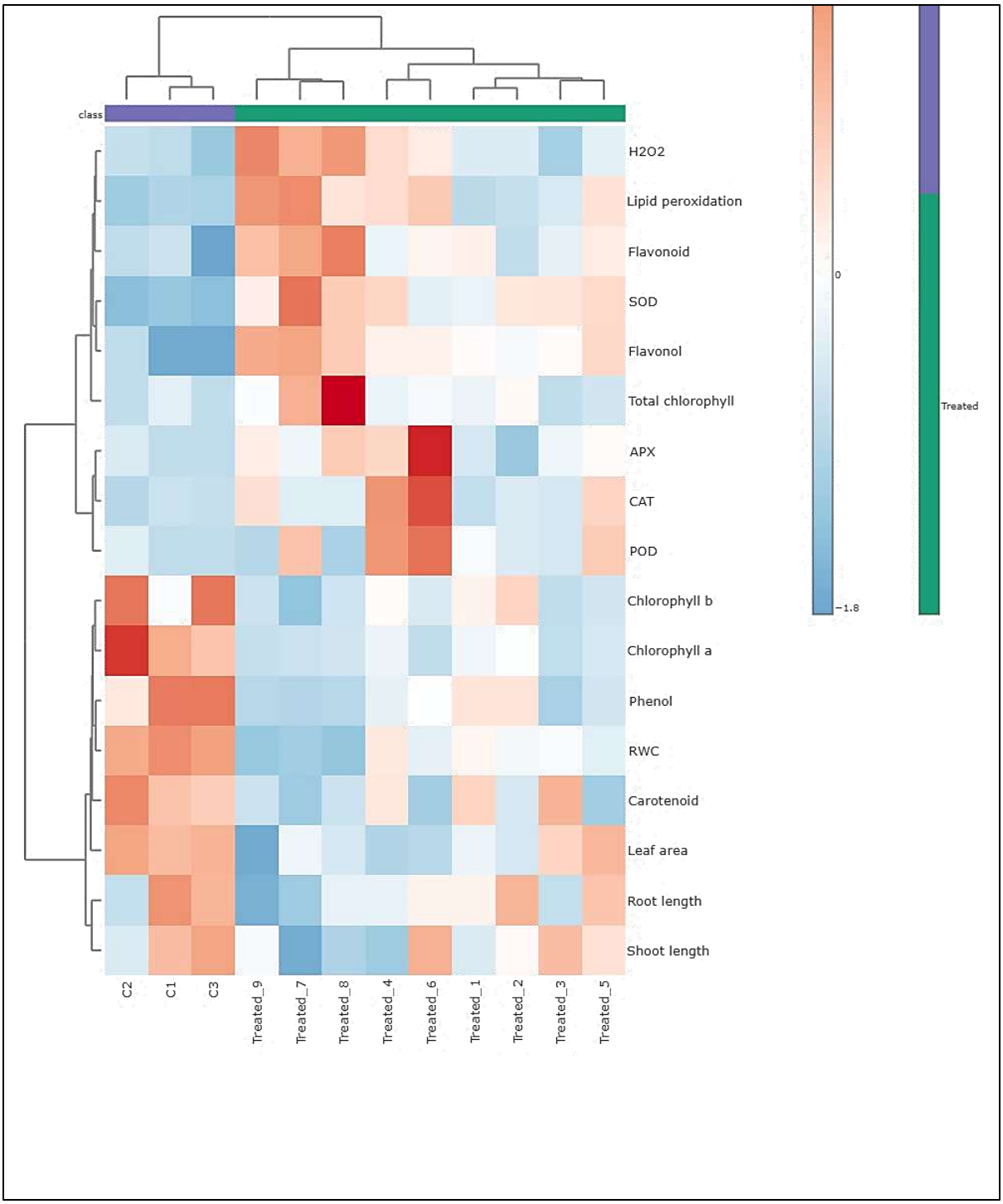


Fig 12: Hierarchical clustering heatmap of physiological, biochemical, and antioxidant parameters in control and PSMP-treated Indian pumpkin plants. Red and blue colors represent relatively higher and lower normalized values, respectively. Samples and variables were clustered using Euclidean distance and Ward's linkage.

4. CONCLUSION

This study demonstrates that the phytotoxic effects of polystyrene microplastics (PSMPs) in *Cucurbita moschata* are driven by a coordinated sequence of physiological and biochemical events initiated at the root–soil interface. Under

soil-like conditions, SEM observations revealed progressive PSMP accumulation on the root surface at lower concentrations, followed by vascular localization at the highest concentration, identifying disruption of root water uptake as the earliest detectable response. The resulting decline in RWC preceded significant growth inhibition and triggered a cascade of stomatal regulation, photosynthetic pigment loss, oxidative stress, activation of enzymatic and non-enzymatic antioxidant defenses, and ultimately lipid peroxidation under severe exposure. Although antioxidant responses effectively buffered oxidative stress at moderate PSMP concentrations, their protective capacity was insufficient to prevent oxidative damage at 0.5 mg mL^{-1}. The exploratory PLS-DA further supported this integrated response, indicating that water status, antioxidant defense, and growth traits were the principal physiological processes associated with PSMP exposure. Collectively, these findings establish disruption of root water relations as the primary physiological driver of PSMP phytotoxicity, with subsequent alterations in photosynthesis, redox homeostasis, secondary metabolism, and growth representing interconnected downstream consequences rather than independent stress responses. By employing a soil-like substrate instead of a hydroponic system, this study provides a more environmentally relevant assessment of PSMP phytotoxicity that accounts for particle–substrate interactions characteristic of terrestrial ecosystems. This work advances the mechanistic understanding of microplastic–plant interactions and provides a conceptual framework for predicting how microplastic contamination may affect crop productivity and resilience under realistic agricultural conditions.

DISCLOSURE OF INTEREST

Authors declare that they don't have any conflict of interest.

DECLARATION OF FUNDING

No funding was received.

REFERENCES

1. Adhikari, A., Balhara, R., Hossain, Z., & Singh, K. (2025). Mechanistic insights into polystyrene nanoplastics (PSMPs) mediated imbalance of redox homeostasis and disruption of antioxidant defense system leading to oxidative stress in black mustard (Brassica nigra L.). Plant Physiology and Biochemistry, 110480.
2. Bai, H., Yang, Y., & Huang, Y. (2024). Distribution of microplastics and their effects on nutrient absorption in strawberry plants. *Scientia horticulturae*, *332*, 113214.
3. Beyer, W. F., & Fridovich, I. (1987). Assaying for superoxide dismutase activity: some large consequences of minor changes in conditions. *Analytical Biochemistry, 161*, 559–566.
4. Biswas, A. U. H., Kamal, T., Akter, A., Akter, S., Bhuiyan, A. R., Moni, Z. A., ... & Islam, F. (2025). Antioxidant and Hepatotoxicity Ameliorative Potential of Mentha canadensis Leaves Against Paracetamol-Induced Hepatic Damage in Mice. *Food Science & Nutrition*, *13*(12), e71279.
5. Brooking, I. R. (1976). Soilless potting media for controlled-environment facilities. New Zealand Journal of Crop and Horticultural Science, 4, 203-208.
6. Bosker, T., Bouwman, L. J., Brun, N. R., Behrens, P., & Vijver, M. G. (2019). Microplastics accumulate on pores in seed capsule and delay germination and root growth of the terrestrial vascular plant *Lepidium sativum*. *Chemosphere*, *226*, 774–781.
7. Caldo, F., Mannino, G., & Maffei, M. E. (2025). Salt stress re-routes terpenoid and flavonoid metabolism in peppermint (*Mentha × piperita* L.). *Physiologia Plantarum*, *177*(6), e70694 Huang
8. Chakraborty, T. K., Rahman, M. S., Nice, M. S., Netema, B. N., Islam, K. R., Debnath, P. C., ... & Munna, A. (2024). Application of machine learning and multivariate approaches for assessing microplastic pollution and its associated risks in the urban outdoor environment of Bangladesh. *Journal of Hazardous Materials*, *472*, 134359.
9. Colzi, I., Renna, L., Bianchi, E., Castellani, M. B., Coppi, A., Pignattelli, S., ... & Gonnelli, C. (2022). Impact of microplastics on growth, photosynthesis and essential elements in Cucurbita pepo L. *Journal of Hazardous Materials, 423*, 127238.
10. Conti, G. O., Ferrante, M., Banni, M., Favara, C., Nicolosi, I., Cristaldi, A., ... & Zuccarello, P. (2020). Micro- and nano-plastics in edible fruit and vegetables. The first diet risks assessment for the general population. *Environmental Research, 187*, 109677.
11. Cui, J., Li, X., Gan, Q., Lu, Z., Du, Y., Noor, I., ... & Jin, B. (2025). Flavonoids mitigate nanoplastic stress in Ginkgo biloba. *Plant, Cell & Environment, 48*, 1790-1811.

12. Cunningham, B. E., Sharpe, E. E., Brander, S. M., Landis, W. G., & Harper, S. L. (2023). Critical gaps in nanoplastics research and their connection to risk assessment. *Frontiers in Toxicology, 5*,1154538.1
13. Daryanavard, H., Postiglione, A. E., Mühlemann, J. K., & Muday, G. K. (2023). Flavonols modulate plant development, signaling, and stress responses. *Current Opinion in Plant Biology, 72*, 102350.
14. Du, Z., & Bramlage, W. J. (1992). Modified thiobarbituric acid assay for measuring lipid oxidation in sugar-rich plant tissue extracts. *Journal of Agricultural and Food Chemistry, 40, 1566-1570.*
15. Dutta Gupta, S., & Datta, S. (2003). Antioxidant enzyme activities during in vitro morphogenesis of gladiolus and the effect of application of antioxidants on plant regeneration. *Biologia Plantarum, 47*, 179–183.
16. Foyer, C. H., & Hanke, G. (2022). ROS production and signalling in chloroplasts: cornerstones and evolving concepts. *The Plant Journal, 111*, 642–661.
17. Gholampoor, M., Osku, M., Jahanifard, M., Sarikhani, S., Aliniaeifard, S., Sadeghi-Majd, R., & Roozban, M. R. (2025). Exploring drought adaptation strategies in pistachios through morpho-physiological analysis under deficit irrigation. *Scientific Reports*.
18. Giorgetti, L., Spanò, C., Muccifora, S., Bottega, S., Barbieri, F., Bellani, L., & Ruffini Castiglione, M. (2020). Exploring the interaction between polystyrene nanoplastics and *Allium cepa* during germination: Internalization in root cells, induction of toxicity and oxidative stress. *Plant Physiology and Biochemistry*, *149*, 170–177.
19. Gong, W., Zhang, W., Jiang, M., Li, S., Liang, G., Bu, Q., Xu, L., Zhu, H., & Lu, A. (2021). Species-dependent response of food crops to polystyrene nanoplastics and microplastics. *The Science of the Total Environment, 796,* 148750.
20. González, L., & González-Vilar, M. (2001). Determination of relative water content. *Handbook of Plant Ecophysiology Techniques,* 207-212.
21. Gupta, S. D., Agarwal, A., & Pradhan, S. (2018). Phytostimulatory effect of silver nanoparticles (AgNPs) on rice seedling growth: An insight from antioxidative enzyme activities and gene expression patterns. Ecotoxicology and environmental safety, 161, 624-633
22. Hosen, M., Rafii, M. Y., Mazlan, N., Jusoh, M., Oladosu, Y., Chowdhury, M. F. N., ... & Khan, M. M. H. (2021). Pumpkin (Cucurbita spp.): a crop to mitigate food and nutritional challenges. *Horticulturae, 7*, 352.
23. Hsiao, T. C., & Xu, L.-K. (2000). Sensitivity of growth of roots versus leaves to water stress: Biophysical analysis and relation to water transport. *Journal of Experimental Botany*, *51*(350), 1595–1616.
24. Hua, Z., Zhang, T., Luo, J., Bai, H., Ma, S., Qiang, H., & Guo, X. (2024). Internalization, physiological responses and molecular mechanisms of lettuce to polystyrene microplastics of different sizes: Validation of simulated soilless culture. *Journal of Hazardous Materials, 462*, 132710.
25. Huang, D., Shi, Z., Shan, X., Yang, S., Zhang, Y., & Guo, X. (2023). Insights into growth-affecting effect of nanomaterials: Using metabolomics and transcriptomics to reveal the molecular mechanisms of cucumber leaves upon exposure to polystyrene nanoplastics (PSMPs). *The Science of the Total Environment, 866*, 161247.
26. Iqbal, R., Khan, M. T., Bilal, H., Aslam, M. M., Khan, I. A., Raja, S., ... & Nguyen, P. M. (2022). Microplastics as vectors of environmental contaminants: Interactions in the natural ecosystems. *Human and Ecological Risk Assessment: An International Journal, 28,* 1022-1042.
27. Islam, F. S. (2025). The effects of plastic and microplastic waste on the marine environment and the ocean. *European Journal of Environment and Earth Sciences, 6*, 1-9.2
28. Jadhav, B., & Medyńska-Juraszek, A. (2024). Microplastic and nanoplastic in crops: possible adverse effects to crop production and contaminant transfer in the food chain. *Plants, 13*, 2526.
29. Jia, L., Liu, L., Zhang, Y., Fu, W., Liu, X., Wang, Q., ... & Huang, L. (2023). Microplastic stress in plants:effects on plant growth and their remediations. *Frontiers in Plant Science, 14,* 1226484.
30. Kar, M., & Mishra, D. (1976). Catalase, peroxidase, and polyphenoloxidase activities during rice leaf senescence. *Plant Physiology, 57*, 315-319.
31. Kochanek, A., Grąz, K., Potok, H., Gronba-Chyła, A., Kwaśny, J., Wiewiórska, I., ... & Lapiński, J.(2025). Micro-and nanoplastics in the environment: current state of research, sources of origin, health risks, and regulations—a comprehensive review. *Toxics, 13*, 564.
32. Kralj, K., & Chen, Z. (2026). A systematic review of micro-and nanoplastics impact on plant photosynthesis. *Journal of Hazardous Materials*, 141776.
33. Kruger, N. J. (2009). The Bradford method for protein quantitation. *The protein protocols handbook*, 17-24.
34. Kumar, D., Biswas, J. K., Mulla, S. I., Singh, R., Shukla, R., Ahanger, M. A., Shekhawat, G. S., Verma, K. K., Siddiqui, M. W., & Seth, C. S. (2024). Micro and nanoplastics pollution: Sources, distribution, uptake in

plants, toxicological effects, and innovative remediation strategies for environmental sustainability. *Plant Physiology and Biochemistry*, *213*, 108795.
35. Kumaran, A., & Karunakaran, R. J. (2007). In vitro antioxidant activities of methanol extracts of five Phyllanthus species from India. *LWT-Food Science and Technology, 40,* 344–352.
36. Li, H., Song, F., Song, X., Zhu, K., Lin, Q., Zhang, J., & Ning, G. (2023). Single and composite damage mechanisms of soil polyethylene/polyvinyl chloride microplastics to the photosynthetic performance of soybean (Glycine max [L.] merr.). *Frontiers in Plant Science, 13*, 1100291.
37. Li, X., Zhang, W., Niu, D., & Liu, X. (2024). Effects of abiotic stress on chlorophyll metabolism. *Plant Science, 342*, 112030.
38. Li, Z., Li, Q., Li, R., Zhao, Y., Geng, J., & Wang, G. (2020). Physiological responses of lettuce (Lactuca sativa L.) to microplastic pollution. *Environmental Science and Pollution Research, 27,* 30306-30314.
39. Lian, J., Wu, J., Xiong, H., Zeb, A., Yang, T., Su, X., ... & Liu, W. (2020). Impact of polystyrene nanoplastics (PSMPs) on seed germination and seedling growth of wheat (Triticum aestivum L.).*Journal of Hazardous Materials, 385*, 121620.
40. Lichtenthaler, H. K. (1987). [34] Chlorophylls and carotenoids: pigments of photosynthetic biomembranes. Methods in Enzymology, 148, 350-382.
41. Lin, J. Y., & Tang, C. Y. (2007). Determination of total phenolic and flavonoid contents in selected fruits and vegetables, as well as their stimulatory effects on mouse splenocyte proliferation. *Food Chemistry, 101*, 140-147.3
42. Liu, B., Li, R., Zhuang, H., Lin, Z., & Li, Z. (2024). Effects of polystyrene microplastics on the phenylpropane metabolic pathway in cucumber plants. *Environmental and Experimental Botany, 220,* 105671.
43. Liu, H., Tang, H., Gao, Y., An, Y., Zhou, J., Li, X., ... & Gou, Z. (2025). The multifaceted mechanisms of microplastic inhibition of tomato plant growth: oxidative toxicity, metabolic perturbation, and photosynthetic damage. *Plant Physiology and Biochemistry,* 110976.
44. Liu, X., Wang, P., An, Y., Wang, C. M., Hao, Y., Zhou, Y., ... & Wang, P. (2022). Endodermal apoplastic barriers are linked to osmotic tolerance in meso-xerophytic grass Elymus sibiricus. *Frontiers in Plant Science, 13*, 1007494.
45. Liu, H., Song, S., Zhang, H., Li, Y., Niu, L., Zhang, J., & Wang, W. (2022). Signaling Transduction of ABA, ROS, and Ca^{2+} in Plant Stomatal Closure in Response to Drought. *International Journal of Molecular Sciences*, *23*(23), 14824.
46. Maity, S., Chatterjee, A., Guchhait, R., De, S., & Pramanick, K. (2020). Cytogenotoxic potential of a hazardous material, polystyrene microparticles on Allium cepa L. *Journal of Hazardous Materials*, *385*, 121560.
47. Maity, S., Guchhait, R., & Pramanick, K. (2024). Role of aquaporins in micro-plastics accumulation in onion roots and the effects of micro-plastics on microtubules stability and organization under heat and salinity stress. *Environmental and Experimental Botany*, *220*, 105692.
48. Mierzejewska-Sinner, E., Urbaniak, M., Inui, H., Thijs, S., & Vangronsveld, J. (2024). Cucurbit plants for remediation of soils polluted with persistent and emerging organic pollutants: State of the art, future perspectives and challenges. *Advances in Botanical Research*, *109*, 217-254.
49. Mousazadehgavan, M. (2026). Microplastics in Aquatic Systems: Dual Roles as Pollutant Carriers and Emerging Functional Materials for Water Treatment. *Water, Air, & Soil Pollution*, *237*(7), 449.
50. Nakano, Y., & Asada, K. (1981). Hydrogen peroxide is scavenged by ascorbate-specific peroxidase in spinach chloroplasts. *Plant and Cell Physiology*, *22*(5), 867–880.
51. Nei, N., Changmai, U., Kumar, N., Borah, B., Chikkaputtaiah, C., Saikia, R., & Phukan, T. (2024). Impact of polyvinyl chloride (PVC) microplastic on growth, photosynthesis and nutrient uptake of Solanum lycopersicum L.(Tomato). *Environmental Pollution, 349,* 123994.
52. Niaz, M., Zhang, B., Zhang, Y., Yan, X., Yuan, M., Cheng, Y., ... & Chen, F. (2023). Genetic and molecular basis of carotenoid metabolism in cereals. *Theoretical and Applied Genetics*, *136*(3), 63.
53. Ninkuu, V., Aluko, O. O., Yan, J., Zeng, H., Liu, G., Zhao, J., ... & Dakora, F. D. (2025). Phenylpropanoids metabolism: Recent insight into stress tolerance and plant development cues. *Frontiers in Plant Science, 16*, 1571825.
54. Ortega, J. K. E. (2025). Theoretical analyses of turgor pressure and expansive growth rate of plant cells during water deficit. *Plants*, *14*(22), 3538
55. Ozfidan-Konakci, C., Yildiztugay, E., Arikan, B., Alp-Turgut, F. N., Turan, M., Cavusoglu, H., & Sakalak, H. (2023). Responses of individual and combined polystyrene and polymethyl methacrylate nanoplastics on

hormonal content, fluorescence/photochemistry of chlorophylls and ROS scavenging capacity in Lemna minor under arsenic-induced oxidative stress. *Free Radical Biology and Medicine*, *196*, 93-107.
56. Parkash, V., Snider, J. L., Virk, G., Dhillon, K. K., & Lee, J. M. (2024). Diffusional and biochemical limitations to photosynthesis under water deficit for field-grown cotton. *Physiologia Plantarum, 176*, Article e14281.
57. Pignattelli, S., Broccoli, A., & Renzi, M. (2020). Physiological responses of garden cress (L. sativum) to different types of microplastics. *Science of the Total Environment, 727*, 138609.
58. Postiglione, A. E., & Muday, G. K. (2020). The role of ROS homeostasis in ABA-induced guard cell signaling. *Frontiers in plant science*, *11*, 968.
59. Ramachandran, P., Ramirez, A., & Dinneny, J. R. (2025). Rooting for survival: how plants tackle a challenging environment through a diversity of root forms and functions. *Plant Physiology, 197*, kiae586.
60. Rao, M. J., & Zheng, B. (2025). The role of polyphenols in abiotic stress tolerance and their antioxidant properties to scavenge reactive oxygen species and free radicals. *Antioxidants, 14*, 74.
61. Rathikannu, S., Gautam, S., Joshi, S. K., Katharine, P., Mithra, K. E., Banusaranya, P., ... & Ho, C. H. (2025). FTIR based assessment of microplastic contamination in soil water and insect ecosystems reveals environmental and ecological risks. *Scientific Reports, 15*, 28615.4
62. Riaz, K., Yasmeen, T., Attia, K. A., Kimiko, I., & Arif, M. S. (2025). Phytotoxic effects of polystyrene microplastics on growth morphology, photosynthesis, gaseous exchange and oxidative stress of wheat vary with concentration and shape. *Toxics, 13*, 57.
63. Sajjad, M., Bahadur, S., Farooq, M. A., & Ren, M. X. (2025). Interactive impacts of heat stress and microplastics contamination on the growth and biochemical response of wheat (Triticum aestivum) and maize (Zea mays) plants. *Ecotoxicology, 34*, 1036-1058.
64. Tardieu, F. (2024). Leaf growth under water-limited conditions. In *Drought adaptation in cereals* (pp. 145-169). CRC Press.
65. Velikova, V., Yordanov, I., & Edreva, A. J. P. S. (2000). Oxidative stress and some antioxidant systems in acid rain-treated bean plants: protective role of exogenous polyamines. *Plant Science, 151,* 59-66.
66. Wang, F., Feng, X., Liu, Y., Adams, C. A., Sun, Y., & Zhang, S. (2022). Micro(nano)plastics and terrestrial plants: Up-to-date knowledge on uptake, translocation, and phytotoxicity. *Resources, Conservation and Recycling*, *185*, Article 106503.
67. Wang, B., Yuan, H., Yang, Y., Jiang, Z., & Xi, D. (2025). Toxicological effects and molecular metabolic of polystyrene nanoplastics on soybean (Glycine max L.): Strengthening defense ability by enhancing secondary metabolisms. *Environmental Pollution (Barking, Essex: 1987), 366*,125522.
68. Wrigley, O., Braun, M., & Amelung, W. (2024). Global soil microplastic assessment in different land-use systems is largely determined by the method of analysis: A meta-analysis. *The Science of the Total Environment, 957*, 177226.
69. Xiao, W., Xiang, P., Liao, W., Xiong, Z., Peng, L., Zou, L., Liu, B., & Li, Q. (2024). Effects of polystyrene microplastics on the growth and metabolism of highland barley seedlings based on LC-MS. *Frontiers in Plant Science, 15*, 1477605.5
70. Xie, Z., Zeng, Y., Zhu, S., Zhu, M., Yu, Y., Cheng, K., & Peng, X. (2026). From energy collapse to chemical defense: Microplastics reshape the metabolic landscape of Tetrastigma hemsleyanum (Vitaceae). *Plant Physiology and Biochemistry*, 111007.
71. Xu, G., Li, X., Zhu, T., Wang, F., & Yin, J. (2025). When nano- and microplastics meet taro (*Colocasia esculenta*) roots: Their size-dependent adsorption, penetration, and promotion on secondary wall reinforcement. *Environmental Science & Technology*, *59*(17), 8345–8356.
72. Yang, Y. J., Bi, M. H., Nie, Z. F., Jiang, H., Liu, X. D., Fang, X. W., & Brodribb, T. J. (2021). Evolution of stomatal closure to optimize water-use efficiency in response to dehydration in ferns and seed plants. *New Phytologist*, *230*(5), 2001-2010.
73. Zantis, L. J., Rombach, A., Adamczyk, S., Velmala, S. M., Adamczyk, B., Vijver, M. G., ... & Bosker, T. (2023). Species-dependent responses of crop plants to polystyrene microplastics. *Environmental Pollution, 335*, 122243.
74. Zhang, Q., Zhao, M., Meng, F., Xiao, Y., Dai, W., & Luan, Y. (2021). Effect of Polystyrene Microplastics on Rice Seed Germination and Antioxidant Enzyme Activity. *Toxics, 9*, 179.
75. Zhishen, J., Mengcheng, T., & Jianming, W. (1999). The determination of flavonoid contents in mulberry and their scavenging effects on superoxide radicals. *Food Chemistry, 64*, 555-559.
76. Zhou, P., Wang, L., Gao, J., Jiang, Y., Adeel, M., & Hou, D. (2023). Nanoplastic–plant interaction and implications for soil health. *Soil Use and Management, 39*, 13-42.

77. Zhuang, H., Chen, L., Wang, N., et al. (2023). Growth and physiological–biochemical characteristics of cucumber (Cucumis sativus L.) in the presence of different microplastics. *Arabian Journal of Geosciences, 16*, 194.
78. Zhu, J., Wang, J., Chen, R., Feng, Q., & Zhan, X. (2022). Cellular process of polystyrene nanoparticles entry into wheat roots. *Environmental Science & Technology*, *56*(10), 6436–6444.

Conflict of Interest

The author declares that there are no conflicts of interest regarding the publication of this manuscript.

NUMBER OF WORDS: 9413

THE NUMBER OF FIGURES: 12

THE NUMBER OF TABLES: 0

Supplementary Files

This is a list of supplementary files associated with this preprint. Click to download.

- Highlights.docx